

CrystEngComm

Accepted Manuscript



This is an *Accepted Manuscript*, which has been through the Royal Society of Chemistry peer review process and has been accepted for publication.

Accepted Manuscripts are published online shortly after acceptance, before technical editing, formatting and proof reading. Using this free service, authors can make their results available to the community, in citable form, before we publish the edited article. We will replace this *Accepted Manuscript* with the edited and formatted *Advance Article* as soon as it is available.

You can find more information about *Accepted Manuscripts* in the [Information for Authors](#).

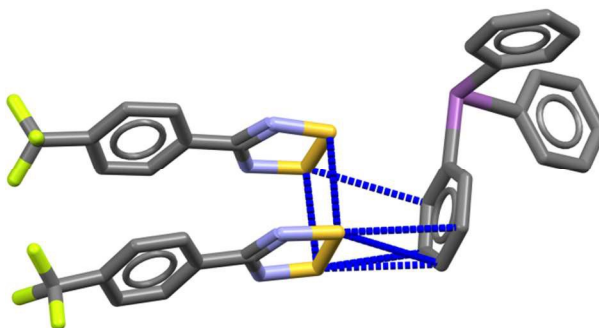
Please note that technical editing may introduce minor changes to the text and/or graphics, which may alter content. The journal's standard [Terms & Conditions](#) and the [Ethical guidelines](#) still apply. In no event shall the Royal Society of Chemistry be held responsible for any errors or omissions in this *Accepted Manuscript* or any consequences arising from the use of any information it contains.

1 **Short contacts of the sulphur atoms of a 1,2,3,5-dithiadiazolyl dimer with**
2 **triphenylstibine: first co-crystal with an aromatic compound †**

3 René T. Boéré*

4 *Department of Chemistry and Biochemistry, and the Canadian Centre for Research in Advanced Fluorine*
5 *Technologies. University of Lethbridge, Lethbridge, Alberta, Canada, T1K 3M4. Fax: +403-329-2057; Tel. +403-*
6 *329-2045 E-mail: boere@uleth.ca*

7 **TOC Graphic and brief text**



8

9 Co-crystallization of aromatic compounds with neutral dithiadiazolyl dimers has not previously succeeded.
10 There is great scope here for crystal engineering using mutually compatible components.

11 **Abstract**

12 The structure of dimeric 2,7-bis[4-(trifluoromethyl)phenyl]-4 λ^4 ,5 λ^4 ,9 λ^4 ,10 λ^4 -tetrathieto[1,2-*a*:3,4-*a'*]bis
13 [1,2,3,5]dithiadiazole (C₈H₄F₃N₂S₂)₂ and its adduct with triphenylstibine, (C₈H₄F₃N₂S₂)₂·C₁₈H₁₅Sb, both have
14 triclinic (*P*1) symmetry. They crystallize in layers containing centrosymmetric clusters consisting of four
15 dithiadiazolyl dimers in the parent compound and two such dimers paired with two triphenylstibine units in the
16 aromatic co-crystal. In the co-crystal, the Ph₃Sb molecules associate with an equivalent moiety from a
17 neighbouring cluster in a geometry that is very reminiscent of other Ph₃Sb-containing structures. Thus, the
18 adduct combines structural elements from those of its component parts. Key interactions between molecules
19 in the pure dithiadiazolyl (S to S) and the co-crystal (S to C) are significantly shorter than the sums of atom van
20 der Waals radii.

21 † Electronic supplementary information (ESI) available: CIF for all X-ray structures have been deposited. CCDC
22 1452129-1452130. For ESI and crystallographic data in electronic format see DOI: 10.1039/xxxx.

23

24 Introduction

25 There is an extensive chemistry of 1,2,3,5-dithiadiazolyl (DTDA) radicals because of interest in metallic
26 conductivity and magnetism.¹ Such properties depend on intermolecular contacts and thus the crystal
27 engineering of DTDA radicals has received intensive investigation.² DTDA radicals normally dimerize in the solid
28 state unless there are both steric factors to prevent dimerization and secondary bonding interactions to
29 stabilize the monomers. There are at least five recognizable dimer configurations; of these the *cis*-oid co-facial
30 is by far the most common. Extensive experimental and theoretical considerations have concluded that the
31 inter-dimer bonds are exclusively between the CN₂S₂ heterocycles and are dominated by S...S interactions,³ a
32 strong interaction that has been effectively described as 'pancake bonding' which constitutes a (diffuse)
33 quantum-chemical bond but also involves a dispersive component and contributions from diradical character.⁴⁻
34 ⁶ Crystal structures have been reported for more than 70 different neutral DTDA dimers and monomers in the
35 Cambridge Structure Database (CSD, Version 5.37, with updates to November 2015).⁷ In only a handful of cases
36 are the structures heterogeneous. A mixed oxidation state species crystallizes as the trimer [5-PhCN₂S₂]₃ (CSD
37 refcode: HEGVOE).⁸ Similarly, a channel structure of HCN₂S₂ crystallizes with ~0.18 iodine atoms in a partial
38 charge-transfer species (refcode LEJFAH).⁹ A co-crystal of PhCN₂S₂ and S₃N₃ involves an indeterminate degree
39 of charge transfer (refcode SIHZAK).¹⁰ The structure of 4-(3-fluoro-4-trifluoromethylphenyl)-1,2,3,5-
40 dithiadiazolyl (refcode: UMAROP) is typical of a (distorted) *cis*-oid dimer, but is significant in the context of this
41 work in that the lattice readily opens up to form channels when co-sublimed with N₂, Ar, CO₂ or SO₂ (refcodes:
42 UMARUV, UMASAC, UMASEG and UMASIK) to form host-guest gas-clathrates.¹¹ This is the only other case to
43 our knowledge where co-crystallization with neutral molecules has previously been demonstrated in DTDA
44 chemistry, although identification of electron density for the incorporated gas molecules relied on the
45 delocalized solvent tools of the PLATON 'SQUEEZE' routine.¹²

46 In two recent reports, Haynes *et al.* and Rawson *et al.* reported on the preparation of fascinating mixed-radical
47 dimers by combining slightly electron rich with electron poorer DTDA's.^{13,14} The successful co-crystallizations
48 include [PhCN₂S₂][5-C₆F₅-CN₂S₂] (refcode: QUNQUM)¹³ and [PhCN₂S₂][NC₅F₅-CN₂S₂] (refcode: YIMNIT),¹⁴ which
49 emphasizes the importance of *perfluorination* for reducing electron richness in DTDA heterocycles via purely
50 inductive effects. Complex charge balances exist in mixed fluorinated/hydrocarbon DTDA dimers, which have
51 been intensively investigated by experimental and computational charge density determinations.³ The co-
52 crystallization could be achieved either from solution or by sublimation in a tube furnace. They also reported
53 many failed attempts by mixing other DTDA's, and attempts to combine about 10 different aromatic ring
54 compounds, incorporating a variety of functional groups, with DTDA's; no co-crystals with aromatics were
55 obtained. It is not clear from the published report as to whether the aromatics were thought to be able to co-
56 dimerize with the DTDA or whether some other form of association was expected. Several recent reports
57 indicate a directive or 'shepherding' role for aromatic co-crystallizers with organic radicals.¹⁵⁻¹⁷ "End-on"
58 interactions from the sulphur atoms of DTDA's with aromatic carbon atoms *belonging to the same DTDA species*
59 have been known since at least 1991. Thus, in the lattice of [1,4-CN₂S₂-C₆H₄]₂ (refcode: VINJIL),¹⁸ there is an
60 interaction between two sulphur atoms of a DTDA dimer and the *ipso* and *ortho* carbon atoms of the di-
61 substituted benzene ring of a neighbouring molecule. It has a shortest C...S contact that is 0.22 Å < Σ*r*_{vdW}. Of
62 much more recent origin are other structures showing similar interactions, as in [3-Cl-4-CH₃-C₆H₃-CN₂S₂]₂
63 (refcode: EZIQUY, shortest C...S contact 0.33 Å < Σ*r*_{vdW}),¹⁹ in [4-F-C₆H₃-CN₂S₂]₂ (refcode: QEFGIT, shortest C...S
64 contact 0.20 Å < Σ*r*_{vdW}),²⁰ in [3-CH₃-C₆H₃-CN₂S₂]₂ (refcode: LELPUP, shortest C...S contact 0.29 Å < Σ*r*_{vdW}),²¹ and in
65 [4-CH₃-C₆H₃-CN₂S₂]₂ (refcode: LELPOJ, shortest C...S contact 0.24 Å < Σ*r*_{vdW}).²¹

66 The synthesis of the fluorinated DTDA radical 5-(4-CF₃C₆H₄)-CN₂S₂, **1** (Chart 1), was reported by Boéré *et al.*²²
 67 and the crystal structure was briefly mentioned in the context of metal coordination chemistry of DTDA
 68 radicals.²³ We now report a detailed analysis of the lattice structure of **1** and the discovery that it can form a
 69 unique 1:1 co-crystal with triphenylstibine, [5-(4-CF₃C₆H₄)-CN₂S₂]₂·Ph₃Sb, **2**, in which a typical *cis*-oid co-facial
 70 radical dimer moiety – in itself of quite similar structure to that found in pure **1** – undergoes specific
 71 supramolecular contacts to a phenyl ring of the stibine. This structure is the first reported co-crystal of DTDA
 72 dimer with an aromatic compound.

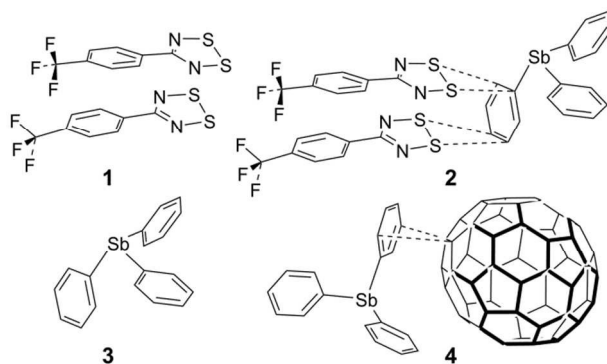


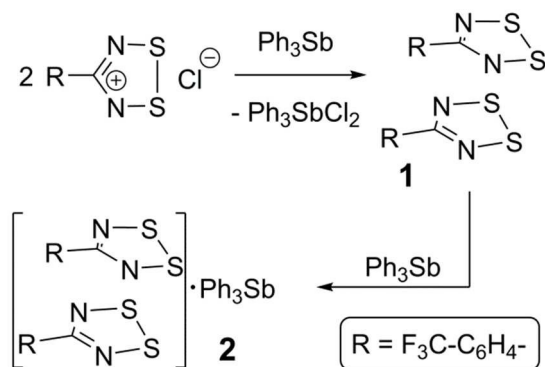
Chart 1

73
74

75 Results and discussion

76 Sample preparation

77 The synthesis of **1** employed triphenylstibine, **3**, as a convenient reducing agent for 1,2,3,5-dithiadiazolium
 78 chlorides and **3** is itself oxidized to Ph₃SbCl₂ (Scheme 1). Because **1** does not precipitate well even from
 79 concentrated CH₃CN solutions, the evaporated crude reaction mixture was directly sublimed in a gradient
 80 sublimator. The neutral radical **1** is more volatile than Ph₃SbCl₂ and is also easy to recognize from its colour. In
 81 the sublimation, **1** presented as dark purple needles which were used for the structure determination. Since
 82 gradient sublimation in vacuum often leads to multiple crystal habits, the presence of dark purple blocks
 83 amongst the needles was not of immediate concern. When the structure of the blocks was solved using the
 84 iterative method of SHELXT²⁴ it was shown to be a 1:1 co-crystal of **1** with **3**. Evidently, some unreacted **3**
 85 was able to sublime and the mixed vapours crystallize to afford **2** in a precise ratio determined by specific
 86 intermolecular interactions. Whereas crude, powdered DTDA samples are very reactive and can inflame in air,
 87 the sublimed crystals of both **1** and **2** are sufficiently stable to handle in air for brief periods (for example,
 88 crystal selection and mounting was done on the open bench.)

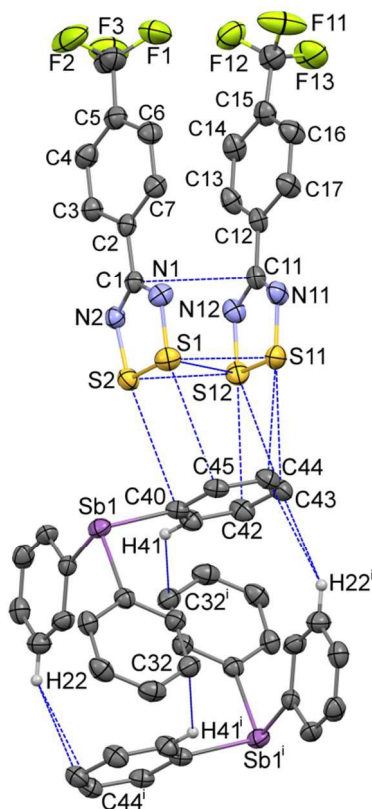


Scheme 1

89
90

91 **Structural commentary and supramolecular features**

92 The geometry of the DTDA dimer in **2** consists of the common *cis*-oid co-facial arrangement of planar CN₂S₂
 93 rings (Figure 1 and Table 1).² Visually, it is indistinguishable from any one of the four independent dimers found
 94 in the crystal structure of **1** (for plots of **1**, see Figure S1 in the ESI; for an overlay structure diagram of dimers
 95 from **1** and **2**, see Figure S2). For clarity and ease of discussion, the atom numbering scheme of the single DTDA
 96 dimer in Figure 1 will be used throughout. The average inter-dimer S...S distance in **2** is 3.068(1) Å, some 0.53 Å
 97 less than the sums of their v.d. Waals' radii (Σr_{vdw}).⁴ The least-squares planes through the two heterocycles that
 98 constitute the dimer in **2** are inclined at 7.87(13)°; in addition the aryl rings twist out of the planes they are
 99 attached to and there is an overall miss-alignment of the upper and lower dimer constituents. Consideration of
 100 3D models indicates that all these effects act to minimize unfavourable steric congestion of the *para*-CF₃
 101 groups on adjacent rings. Such a distortion is also evident in all four dimers in the asymmetric unit of **1**, which
 102 crystallizes in the same space group, *P*1, but with *Z* = 16 rather than two (see the Experimental section for
 103 details). In **1**, each dimer has a slightly different manifestation of steric distortions to accommodate the bulky
 104 CF₃ groups; the average tilt angles for the four dimer pairs is 6.1(8)° from which the value in **2** cannot be
 105 differentiated at the 99% confidence level. If for the miss-alignment of the dimer components we take the
 106 torsion angle C5-C1-C11-C15, the range for **1** is 2.7(1) - 5.6(1)°, within which the value of 3.0(8)° for **2** fits
 107 comfortably. The average inter-dimer S...S distance for the four dimers in **1** is 3.07(5) Å, or 0.53(5) Å less than
 108 Σr_{vdw} .



109

110 **Figure 1.** Displacement ellipsoids (30% probability level) of the 263 K structure of **2**, depicting the asymmetric
 111 unit augmented by the symmetry-equivalent second component of the *pseudo*-cuboidal Ph₃Sb entity, showing
 112 the atom numbering scheme used to discuss both **1** and **2**. Intermolecular contacts up to ($\Sigma r_{vdw} + 0.1$) Å are
 113 shown by dotted lines. [Symmetry code: (i) 2 - x, -y, 1 - z.] The CF₃ groups are rotationally disordered (see ESI).

114 **Table 1.** Selected DTDA interatomic distances (Å) and angles (°) from the crystal structures of **1** - **3**.

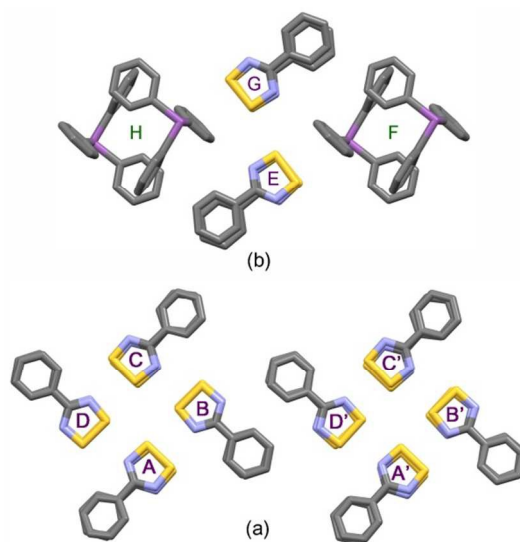
Parameter ^a	1 -i ^b	1 -ii ^c	1 -iii ^d	1 -iv ^e	2
S1—S2	2.0886(18)	2.0879(18)	2.0881(19)	2.0784(19)	2.0865(9)
S1—N1	1.622(4)	1.636(4)	1.626(4)	1.628(4)	1.629(2)
S2—N2	1.626(4)	1.624(4)	1.625(4)	1.622(4)	1.629(2)
N1—C1	1.338(6)	1.336(6)	1.328(6)	1.346(6)	1.336(3)
N2—C1	1.342(6)	1.339(6)	1.330(6)	1.337(6)	1.330(3)
C1—C2	1.476(6)	1.469(6)	1.485(7)	1.474(6)	1.479(3)
S11—S12	2.0840(19)	2.0798(18)	2.0753(18)	2.0841(18)	2.0972(10)
S11—N11	1.633(4)	1.639(4)	1.628(4)	1.639(4)	1.626(2)
S12—N12	1.634(4)	1.621(4)	1.636(4)	1.621(4)	1.629(2)
N11—C11	1.337(6)	1.339(6)	1.339(6)	1.338(6)	1.339(3)
N12—C11	1.333(6)	1.339(6)	1.339(6)	1.336(6)	1.334(3)
C11—C12	1.478(6)	1.483(6)	1.480(6)	1.485(6)	1.485(4)
N1—S1—S2	94.27(16)	94.67(16)	94.01(16)	95.21(16)	94.40(8)
N2—S2—S1	94.60(15)	94.16(15)	94.63(16)	94.59(16)	94.42(8)
C1—N1—S1	115.0(3)	114.0(3)	114.6(3)	113.1(3)	114.27(18)
C1—N2—S2	114.4(3)	114.9(3)	114.0(3)	114.2(3)	114.39(17)
N2—C1—N1	121.7(4)	122.1(4)	122.8(4)	122.8(4)	122.5(2)
N2—C1—C2	117.1(4)	119.3(4)	118.2(4)	118.9(4)	118.7(2)
N1—C1—C2	121.2(4)	118.5(4)	119.0(4)	118.2(4)	118.7(2)
N11—S11—S12	94.19(16)	94.96(15)	94.25(16)	94.80(15)	94.56(8)
N12—S12—S11	94.91(15)	94.50(15)	95.21(15)	94.28(16)	94.12(8)
C11—N11—S11	114.4(3)	113.3(3)	114.8(3)	113.6(3)	114.21(19)
C11—N12—S12 ^e	113.7(3)	114.6(3)	113.5(3)	115.0(3)	114.57(19)
N12—C11—N11	122.8(4)	122.6(4)	122.3(4)	122.3(4)	122.5(2)
N12—C11—C12	118.9(4)	117.9(4)	120.7(4)	117.2(4)	119.1(2)
N11—C11—C12	118.3(4)	119.5(4)	117.0(4)	120.4(4)	118.4(2)
	3a -i ^f	3a -ii ^f	3b -i ^g	3b -ii ^g	2
Sb1—C20	2.143(6)	2.155(6)	2.146(5)	2.154(7)	2.146(5)
Sb1—C30	2.150(10)	2.170(10)	2.143(7)	2.148(7)	2.143(7)
Sb1—C40	2.151(9)	2.161(9)	2.139(8)	2.139(7)	2.139(8)
C20—Sb1—C30	98.0(3)	95.2(3)	96.5(3)	96.1(3)	97.46(9)
C20—Sb1—C40	95.7(3)	95.5(3)	96.5(2)	97.4(3)	96.88(9)
C30—Sb1—C40	96.0(3)	97.5(3)	96.0(3)	95.5(3)	95.76(9)
$\sum \angle(\text{C-Sb-C})$	289.7(4)	288.2(4)	289.0(3)	289.0(4)	290.1(11)

115 ^a The atom numbering scheme is that of **2**, see Figure 1. ^b Dimer i: S1S2;S3S4. ^c Dimer ii: S5,S6;S7S8. ^d Dimer iii:
116 S9,S10;S11S12. ^e Dimer iv: S13,S14;S15S16. ^f CSD refcode: ZZZEA01; 2 mol. per eq. pos.²⁵ ^g CSD refcode:
117 ZZZEA02; 2 mol. per eq. pos.²⁶

118 Within the heterocycles, the average S—S bond length of 2.0919(9) Å in **2** (Table 1) can be compared to a mean
119 of 2.085(3) Å for four such bonds in **1**; the average S—N bond length of 1.628(1) Å with a mean of 1.629(7) Å in

120 **1**; the average N1–C1 bond length of 1.335(3) Å with a mean of 1.338(3) Å in **1** and the average C1–C2 bond
 121 length of 1.482(3) Å with a mean of 1.477(5) Å in **1**. Each parameter in **2** is therefore comfortably within the
 122 statistical ranges observed for the independent values found in the structure of **1** except the S–S bond length
 123 which is *statistically* longer in **2**; however, the difference is just 0.3%, so is unlikely to be chemically significant.

124 Triphenylstibine, **3**, is a long-known compound; structures have been reported in triclinic (refcode: ZZZEHA01)
 125 ²⁵ and monoclinic (refcode: ZZZEHA02) polymorphs,²⁶ both of which have two independent molecules per
 126 asymmetric unit. The Ph₃Sb geometry is remarkably uniform amongst all of these structures (Table 1). Thus the
 127 mean Sb–C distance in **2** of 2.153(6) Å is well within the s.u. of the mean values for the five independent
 128 molecules in the comparison set at 2.150(8) Å, whilst the mean C–Sb–C pyramidal angles in **2** at 96.7(7)° is also
 129 within s.u. of 96.3(8)° in the comparison set. The close-to-90° angles at antimony, which is a feature of heavy
 130 Group 15 element chemistry, are possibly of importance for stabilizing the *pseudo*-cuboidal dimerization of
 131 Ph₃Sb also depicted in Figure 1. This geometry is almost indistinguishable from that in the monoclinic form of **3**
 132 (see Figure S7 in the ESI). The shortest contacts are “T-interactions” from a ring C atom to a CH of the other
 133 component, with lengths in **2** and **3** of 2.915 and 2.862 Å. This association of two strongly pyramidal triphenyl
 134 components is reminiscent of the supramolecular organization of Ph₄P⁺ cations which has been dubbed the
 135 “sextuple phenyl embrace” with an estimated attraction energy of 60–85 kJ·mol⁻¹.²⁷



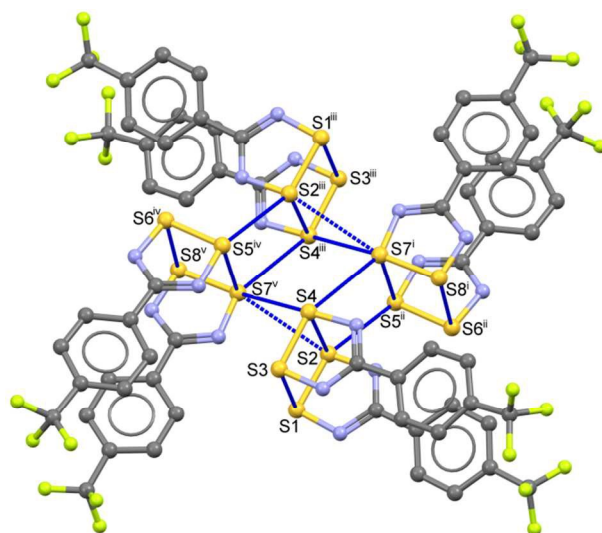
136

137 **Figure 2.** Simplified “cartoons” depicting the arrangements of clusters within one double-layer, which occur in
 138 the crystal lattices of **1** (a) and **2** (b); for detailed diagrams of these layers see the ESI (Figures S3 and S5).

139 The supramolecular architecture of **1**, beyond its *cis*-oid dimerization,⁴ is dominated by a ‘pin-wheel’
 140 arrangement of four such DTDA dimers into a square pattern, with short inter-molecular contacts between
 141 dimers, from the ‘end’ of one set to the ‘side’ of the next, continuing around the square. To start the
 142 discussion, consider the simplified diagram in Figure 2. There are *two* such sets of *centrosymmetric* pin-wheels,
 143 (A± D) and (A'± D'), each composed of four different monomers that are symmetry duplicated. Thus, in Figure
 144 2a, dimers A and C are the same two molecules but reversed in this top-down view, as are B and D; the second
 145 pinwheel is similarly composed of A'/C' and B'/D'. This type of pin-wheel motif has been observed in several
 146 DTDA crystal structures;² it is most common for structures that adopt the tetragonal space group *I*₄₁/*a*.
 147 Examples include [2,6-F₂-C₆H₃-CN₂S₂]₂ (refcode: VUXZEU02),²⁸ [2,5-F₂-C₆H₃-CN₂S₂]₂ (refcodes: NIHBAH and

148 NIHBAH01),^{29,30} and [1,3-(S₂N₂C)₂-C₆H₄]₂ (refcode: SOBSOR).³¹ There is one report of pin-wheels in space group
 149 *I*42*m*, [1,3-CN₂S₂-5-^tBu-C₆H₃]₂ (refcode: POYXAC).³² The lattice of **1** appears as if it should be tetragonal (i.e.
 150 thereby rendering the two pin-wheels equivalent) but it is undoubtedly the distortions induced by the bulky CF₃
 151 groups that frustrate full adoption of such symmetry. Indeed, there are precedents for this too: in [1,3,5-
 152 (S₂N₂C)₃-C₆H₃]₂, pin wheels exist in space group *P*2₁/*c* although its lattice is metrically close to tetragonal
 153 (refcode: KUFDUK),³³ whilst in [3,5-Cl₂-C₆H₃-CN₂S₂]₂ (refcode: DIXNEF) in space group *P*1, the lattice contains a
 154 mixture of tetrameric pin-wheels of dimers and isolated doublets of dimers.³⁴

155 The most remarkable supramolecular feature of **2** is the series of 'end-on' short contacts between the four
 156 sulphur atoms of the DTDA dimer and the aryl ring atoms C42-C45, which range from 3.168(3) - 3.463(3)Å [0.33
 157 to 0.04 Å < Σr_{vdw}] as shown in Figure 1. All of these carbon atoms are part of one phenyl ring belonging to a
 158 Ph₃Sb and the mutual orientation of the components in **2** precludes interaction with the antimony donor
 159 electron pair. There are additional aryl ring "T-interactions" between the DTDA aryl H atoms and ring carbon
 160 atoms of the stibine, which results in an alternating pattern of (DTDA)₂± Ph₃Sb± (DTDA)₂± Ph₃Sb which,
 161 although somewhat rectangular, strongly resembles the pin-wheel arrays in **1** (Figure 2b). This cluster is also
 162 centrosymmetric, so that dimer G is the inverse of E, and H the inverse of F. In both structures, the assemblies
 163 occur within well-defined layers. Thus, one way to describe the supramolecular architecture of **2** is that Ph₃Sb
 164 molecules, each also part of their own *pseudo*-cuboidal dimers, replace every second DTDA dimer specifically
 165 at the site of the "end-on" bonding (Figure 2b).

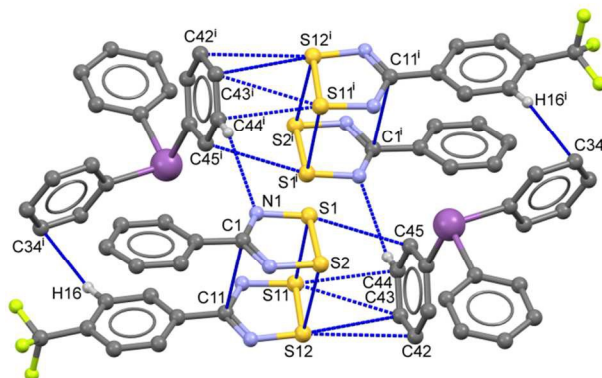


166

167 **Figure 3.** One of two symmetry-independent, centrosymmetric, pin-wheel clusters in the asymmetric unit of **1**
 168 showing intermolecular contacts shorter than ($\Sigma r_{vdw} - 0.2$ Å). H atoms have been removed to enhance visibility.
 169 [Symmetry codes: (i) *x*, -1+*y*, *z*; (ii) 1+*x*, -1+*y*, *z*, (iii) 1+*x*, -1+*y*, *z*, (iv) -*x*, 1-*y*, 1-*z*, (v) 1-*x*, 1-*y*, 1-*z*.] The CF₃ groups
 170 belonging to molecules *iv* and *v* are rotationally disordered (for details, see the ESI).

171 In Figure 3, one of the two essentially equivalent pin-wheels in the structure of **1** is shown in molecular detail.
 172 For a more extended view of the lattice, please see the ESI (Figure S3), where several sets of the two
 173 symmetry-independent pin-wheels are depicted from a top view and a side view. The latter emphasizes the
 174 "double-layer" structure consisting of slices of the lattice that are parallel to the (1 1 0) Miller planes and are
 175 about 8.3 Å thick. Metric data for the intermolecular contacts both between the monomers and between the

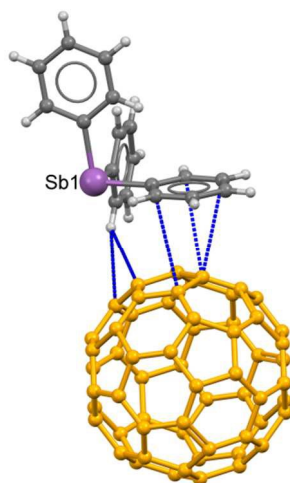
176 dimers that are shown in Figure 3 are available in Table S1 (for a different perspective, see Figure S4 in ESI).
 177 Noteworthy is the relative shortness of all these contacts, i.e. all the blue lines in Figure 3 are from contacts
 178 shorter than ($\Sigma r_{vdw} - 0.2 \text{ \AA}$). By contrast, the pin-wheels in the slices above and below the one that is drawn in
 179 Figure S3 are partly offset and the shortest contacts from one slice to the next are S3...S5' at 3.711(2) and
 180 S10...S14' at 3.765(2) \AA , much weaker interactions that are *longer* than Σr_{vdw} .



181

182 **Figure 4.** Unit cell contents of the centrosymmetric crystal structure of **2** showing intermolecular contacts
 183 shorter than Σr_{vdw} . H atoms except those involved in contacts and the CF₃ groups on front upper and back
 184 lower DTDA have been removed to enhance visibility. [Symmetry code: (i) 1-x,1-y,1-z.]

185 Similarly, Figure 4 presents a more detailed view of the intermolecular contacts that support the
 186 supramolecular architecture of the crystal lattice of **2**. A more extended view of the lattice and a side-view is
 187 provided in the ESI (Figure S5) Metric data for the intermolecular contacts shown by the blue dotted-lines in
 188 Figure 4 are reported in Table S2. Noteworthy here is that the shortest sulphur-carbon interaction of 3.168(3) \AA
 189 is as short when expressed as (distance < Σr_{vdw}) to the sulphur-sulphur inter-molecular contacts in **1** (see Tables
 190 S1 and S2 in the ESI), i.e. they appear to be of comparable strength.



191

192 **Figure 5.** Interaction of a Ph₃Sb phenyl ring with a 6:5 junction bond of C₆₀ in the adduct structure (refcode:
 193 YIKVET).¹⁹ The carbon atoms in the fullerene are rendered orange for contrast.

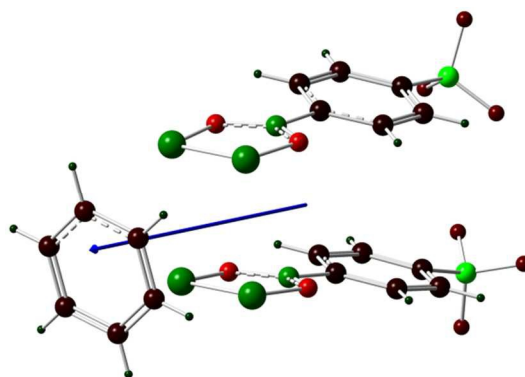
194 For the sole other example of supramolecular interactions to Ph₃Sb of the type observed in **2** we must turn
 195 (Figure 5) to a co-crystal with fullerene, **4**. This structure (refcode: YIKVET)³⁵ displays a side-on interaction from

196 the face of one of the three phenyl rings over a 6:5 ring junction of C_{60} (there are altogether six Ph_3Sb
 197 associated with each C_{60} molecule, see the ESI, Figure S6). The contact distances are on the order of the Σr_{vdW}
 198 ($3.48(1) - 3.65(1) \text{ \AA}$) and were attributed to an electrostatic interaction between a region of partial negative
 199 charge in the center of the phenyl ring and a region of partial positive charge on the C_{60} surface,³⁵ although
 200 there is almost certainly a significant contributions from dispersion. To test this hypothesis, a PBEPBE/6-
 201 311+g(2df,2p) DFT calculation was undertaken (see Figure S8 and Table S4, ESI) on a somewhat simplified
 202 model. The average NPA charge of the (model) benzene C atoms is $-0.183 e$ and of the 6:5 junction C atoms is
 203 $+0.006$, so that Δq is $0.189 e$. When a similar calculation is performed on a model system for **2**, the sulphur
 204 atoms bear an average NPA charge of $+0.465 e$ (Figure 6 and Table 2) and the average benzene C charge is -
 205 $0.182 e$, so that Δq is $0.647 e$. The net dipole moment of 6.9 Debye is oriented along the middle of the DTDA
 206 dimer and is directed to the benzene ring face.

207 **Table 2.** Compilation of computed NPA atomic charges in the model system for **2**^a

Atom	Charge	Atom	Charge
S1	0.463	C8	1.010
S2	0.467	F1	-0.317
N1	-0.716	F2	-0.323
N2r	-0.705	F3	-0.347
C1	0.497	C40	-0.203
C2	-0.114	C41	-0.173
C3	-0.135	C42	-0.170
C4	-0.158	C43	-0.179
C5	-0.107	C44	-0.182
C6	-0.160	C45	-0.187
C7	-0.130		

208 ^a Data taken from PBEPBE/6-311+g(2df,2p) DFT calculation. A full listing is provided in Table S3, ESI.



209

210 **Figure 6.** Computed NPA atomic charges from a PBEPBE/6-311+g(2df,2p) DFT calculation and the net dipole
 211 moment of a model structure in which the pendant Ph_2Sb group has been removed. Red indicates regions of
 212 negative charge and green is positive.

213 Experimental

214 General

215 Unless otherwise indicated, all procedures were performed under an atmosphere of purified N₂ using a
216 glovebox, Schlenkware, and vacuum-line techniques. Solvents used were reagent-grade or better. Acetonitrile
217 (HPLC grade) was double-distilled from P₂O₅ and CaH₂ and diethyl ether was distilled from
218 sodium/benzophenone. SCl₂ was distilled under protection from moisture (5 mL crude containing 1 mL PCl₃),
219 stored on ice, and used within a few hours. Infrared spectra were obtained as Nujol mulls between CsI plates
220 and were recorded on a Bomem MB102 Fourier transform spectrometer. Melting points (capillaries) were
221 determined on an Electrothermal melting point apparatus and are uncorrected. Combustion analysis was
222 performed by M-H-W Laboratories, Phoenix, AZ. Gradient sublimation was undertaken using a home-build 3-
223 zone tube furnace under dynamic vacuum for initial purification followed by slow sublimation in a sealed,
224 evacuated Pyrex tube (15 mm i.d. × 600 mm). The zone temperatures were adjusted based on visual inspection
225 of the progress of sublimation. The silylated amidine 4-F₃CC₆H₄C(=NTMS)N(TMS)₂ was prepared by the
226 literature method.³⁶

227 Preparation of 1

228 In a typical preparation, 5.0 g (13.5 mmol) of 4-F₃CC₆H₄C(=NTMS)N(TMS)₂ was warmed into 40 mL of CH₃CN,
229 whereupon excess, freshly distilled, SCl₂ (2 mL, excess) was added through the top of a reflux condenser with
230 vigorous agitation. After several hours refluxing, the solution was cooled to ambient and filtered under inert
231 gas. The dried 4-F₃CC₆H₄CN₂S₂⁺Cl⁻ was re-suspended in a minimum quantity of warm acetonitrile, freeze-thaw
232 degassed 3×, and then 2.5 g solid Ph₃Sb (7 mmol, slight excess based on the amidine) was added from a solids
233 addition funnel. After refluxing for 30 min, the solution was cooled to ambient after which volatiles were
234 removed using vacuum. The dried cake was transferred (*caution*: glove box!) to a borosilicate glass sublimation
235 tube (20 mm i.d. × 600 mm) and sublimed in a dynamic vacuum in a horizontal tube furnace. The crude, black,
236 sublimed material was then placed in a narrower tube, evacuated and sealed by melting the constricted neck.
237 Careful gradient sublimation using three heating zones resulted in some colourless crystals near the origin and
238 well-formed but small needles amongst large blocks of purple to black crystals. Crystals were harvested in a
239 glove box by sacrificing the glass tube.

240 X-ray Crystallography

241 A thin, dark purple-black, needle corresponding to **1** was selected, coated in Paratone™ oil, mounted on the
242 end of a thin glass capillary and cooled on the goniometer head to 173(2) K with the Bruker low-temperature
243 accessory. A large red-purple block corresponding to **2** was likewise selected and mounted, but the best
244 dataset could be obtained at 263(2) K. A full hemisphere of data was collected for each on a Bruker APEX-II
245 diffractometer using Mo K α radiation ($\lambda = 0.71073 \text{ \AA}$) controlled by APEX2 software.³⁷ A multi-scan absorption
246 correction (SADABS)³⁷ was applied to the data, scaled and corrected for polarization (SAINT-Plus),³⁷ where
247 after the structure was solved by direct methods (SHELXS or SHELXT)^{24,38} and refinement was conducted with
248 full-matrix least-squares on F^2 using SHELXL-2014.³⁹ H atoms attached to carbon were observed in a fine-
249 focused Fourier map and were treated as riding on their attached aromatic carbon atoms with C–H = 0.95 Å
250 and $U_{\text{iso}} = 1.2U_{\text{eq}}(\text{C})$ for the purpose of model refinement. The structure of **1** has disorder of the CF₃ groups in
251 one of four independent DTDA dimers. An adequate two part disorder model was developed; restraints were
252 required to ensure adequate geometries. For a detailed description and graphics, see the ESI (Figure S9). The
253 structure of **2** displays a similar disorder applying to both CF₃ groups for which a model akin to that used for **1**
254 was developed. Details are in the ESI (Figure S10). In the refinement of both structures, the displacement
255 ellipsoids were globally restrained using the newly developed RIGU code in SHELX-2014.^{39,40} This was necessary

256 to prevent oblate or NPD fluorine displacement ellipsoids and was also valuable for the increased thermal
 257 motion in the structure of **2** determined at 263 K. Crystal and experimental parameters are compiled in Table 3,
 258 and selected interatomic distances are available in Table 1. More detailed crystal structure reports are
 259 available in Tables S5 & S6, ESI. Structures were visualized and the lattice geometrical properties were analyzed
 260 with the use of Mercury v3.7.⁴¹ Structure depositions: **1**, CCDC 1452129 and **2** CCDC 1452130, contain the
 261 supplementary crystallographic data for this paper. These data can be obtained, free of charge, via
 262 <http://www.ccdc.cam.ac.uk/products/csd/request/> (or from the Cambridge Crystallographic Data Centre, 12
 263 Union Road, Cambridge CB2 1EZ, U.K. (Fax: 44-1223-336033 or e-mail: deposit@ccdc.cam.ac.uk)).

264 **Table 3.** Crystal, structure determination and refinement parameters

Parameter	1	2
Formula	C ₈ H ₄ F ₃ N ₂ S ₂	C ₃₄ H ₂₃ F ₆ N ₄ S ₄ Sb
FW (amu)	249.25	851.55
Temperature (K)	173(2)	263(2) K
Radiation, λ (Å)	Mo, 0.71073	Mo, 0.71073
Crystal system	Triclinic	Triclinic
Space group	P1	P1
<i>a</i> (Å)	9.4916(9)	11.4543(10)
<i>b</i> (Å)	18.1887(17)	11.7399(10)
<i>c</i> (Å)	22.275(2)	13.9480(12)
α (°)	91.5790(10)	73.3640(10)
β (°)	97.3290(10)	73.2470(10)
γ (°)	102.7550(10)	82.5790(10)
Volume (Å ³)	3713.8(6)	1718.6(3)
Z	16	2
D _{calc} (g/cm ³)	1.783	1.646
μ (mm ⁻¹)	0.583	1.110
F(000)	2000	848
Crystal size (mm ³)	0.18 x 0.10 x 0.04	0.460 x 0.420 x 0.280
θ range (°)	1.847 to 26.220	1.813 to 28.578°
Index ranges:	-11 ≤ <i>h</i> ≤ 11 -22 ≤ <i>k</i> ≤ 22 -27 ≤ <i>l</i> ≤ 27	-15 ≤ <i>h</i> ≤ 15 -15 ≤ <i>k</i> ≤ 15 -18 ≤ <i>l</i> ≤ 18
Total rfl.	39140	19773
Indep. rfl.	14828	8041
R(int)	0.0812	0.0195
Compl. θ 25.5°	99.6 %	99.6 %
Abs. corr.	Semi-empirical from equivalents	
Max. and min. transmission	0.900 0.811	0.900 0.717
Data / restraints / parameters ^a	14828 / 1034 / 1137	8041 / 594 / 516
GOF, <i>F</i> ²	0.973	1.054
Final R indices [<i>I</i> > 2 σ]	R ₁ = 0.0540, wR ₂ = 0.0930	R ₁ = 0.0313, wR ₂ = 0.0789
R indices (all data)	R ₁ = 0.1396, wR ₂ = 0.1185	R ₁ = 0.0404, wR ₂ = 0.0864
Larg. pk (e/Å ⁻³)	0.470	0.664
Larg. hole (e/Å ⁻³)	-0.456	-0.590

^a Full-matrix least-squares on *F*².

265

266 Computation

267 For the DFT calculations, a simplified model with benzene representing the phenyl group of **2** was employed,
268 using the crystal structure geometry to define the shape. The pendant Ph₂Sb group was removed and replaced
269 by an H atom at standard C–H distances using the program GaussView 5.0. A density functional theory (DFT)
270 calculation was undertaken at this static geometry at the PBEPBE/6-311+G(2df,2p) level of theory in Gaussian
271 W03 on a personal computer under Windows 7.⁴² The lack of availability of good parameters for antimony in
272 high-level basis sets was the main reason for excluding it from these calculations. The Normal Population
273 Analysis atomic charges and the calculated dipole moment were visualized in GaussView (Figure 7). In an
274 analogous fashion, a model of C₆₀ surrounded by a hexagonal array of six benzene rings in the location of Ph₃Sb
275 phenyl rings was computed as a model for **4** (see ESI, Figure S8 and Table S4).

276 Conclusions

277 Co-sublimation of rather volatile 4-CF₃-substituted DTDA **1** with triphenylstibine **3** results in a well-defined 1:1
278 adduct **2** that is linked by supramolecular contacts between the electropositive heterocycle sulphur atoms and
279 the negative charge associated with the phenyl ring π -system. The structure determined for **2** shows
280 remarkable similarity to that of the parent DTDA dimer; in place of the ‘pin-wheel’ arrangement of four such
281 dimers in the lattice of **1**, the adduct shows two DTDA dimers and two Ph₃Sb unit, resulting in a slightly
282 rectangular arrangement in place of the symmetrical square. The aromatic interactions do not disrupt the
283 ‘pancake bonding’ within DTDA dimers, but involve the sulphur terminus of the rings in a longitudinal
284 interaction of a type that dominates DTDA crystal engineering.² A preliminary investigation of NPA charges
285 shows a significantly larger electrostatic component to the interaction in **2** compared to the C₆₀ adduct **4**,
286 consistent with shorter intermolecular contact distances in **2** compared to **4**.

287 Ph₃Sb may be a very suitable complexing agent for many thiazyl radicals;³⁵ the resulting supramolecular
288 architectures may be capable of further optimization to achieve desirable solid-state properties. Further
289 progress in DTDA-aromatic supramolecular chemistry may be anticipated by concentrating on very electron
290 rich aromatics – mesitylene or durene as benzene derivatives – but also PAHs such as triphenylene⁴³ or
291 perylene. By employing *radical aromatics* such as phenalenyl, it may indeed be possible to engineer mixed
292 DTDA/aromatic pancake dimers.^{44,45}

293 Acknowledgements

294 The Natural Sciences and Engineering Research Council of Canada (NSERC) is gratefully acknowledged for
295 generous support through the Discovery Grants program. The diffractometer was purchased with the help of
296 NSERC and the University of Lethbridge. Many students have worked on dithiadiazolyl chemistry in my
297 laboratory over the years. Their names appear in the cited references. The anonymous referees are thanked for
298 several helpful suggestions.

299 References

- 300 1. R. T. Boéré and T. L. Roemmele, “Chalcogen–Nitrogen Radicals”. In: Jan Reedijk and Kenneth
301 Poeppelmeier, editors. *Comprehensive Inorganic Chemistry II*, 2013, Vol 1. Oxford: Elsevier. p. 375- 411.
- 302 2. D. A. Haynes, *CrystEngComm*, 2011, **13**, 4793–4805.

- 303 3. S. Domagala, K. Kosci, S. W. Robinson, D. A. Haynes and K. Woźniak, *Cryst. Growth Des.*, 2014, **14**, 4834–
304 4848.
- 305 4. K. E. Preuss, *Polyhedron*, 2014, **79**, 1–15.
- 306 5. H. Z. Beneberu, Y-H. Tian and M. Kertesz, *Phys. Chem. Chem. Phys.*, 2012, **14**, 10713–10725.
- 307 6. R. T. Oakley, *Prog. Inorg. Chem.*, 1988, **36**, 299–391
- 308 7. F. H. Allen, *Acta Cryst.* 2002, **B58**, 380–388.
- 309 8. C. D. Bryan, A. W. Cordes, R. C. Haddon, R. G. Hicks, R. T. Oakley, T. T. M. Palstra, A. S. Perel and S. R. Scott,
310 *Chem. Mater.* 1994, **6**, 508–515.
- 311 9. C. D. Bryan, A. W. Cordes, R. C. Haddon, R. G. Hicks, D. K. Kennepohl, C. D. MacKinnon, R. T. Oakley, T. T.
312 M. Palstra, A. S. Perel, S. R. Scott, L. F. Schneemeyer and J. V. Waszczak, *J. Am. Chem. Soc.* 1994, **116**,
313 1205–1210.
- 314 10. A. J. Banister, M. I. Hansford, Z. V. Hauptman, A. W. Luke, S. T. Wait, W. Clegg and K. A. Jorgensen, *J. Chem.*
315 *Soc. Dalton Trans.* 1990, 2793–2808.
- 316 11. C. S. Clarke, D. A. Haynes, J. M. Rawson and A. D. Bond, *Chem. Commun.*, 2003, 2774–2775.
- 317 12. A. L. Spek, *Acta Crystallogr. C. Struct. Chem.*, 2015, **71**, 9–18.
- 318 13. C. Allen, D. A. Haynes, C. M. Pask, and J. M. Rawson, *CrystEngComm*, 2009, **11**, 2048–2050.
- 319 14. S. W. Robinson, D. A. Haynes and J. M. Rawson, *CrystEngComm*, 2013, **15**, 10205–10211.
- 320 15. H. Akpınar, J. T. Mague and P. M. Lahti, *CrystEngComm*, 2013, **15**, 831–835.
- 321 16. G. M. Espallargas, A. Recuenco, F. M. Romero, L. Brammer and S. Libri, *CrystEngComm*, 2012, **14**, 6381–
322 6383.
- 323 17. H. Akpınar, J. T. Mague, M. A. Novak, J. R. Friedman and P. M. Lahti, *CrystEngComm*, 2012, **14**, 1515–1526.
- 324 18. A. W. Cordes, R. C. Haddon, R. T. Oakley, L. F. Schneemeyer, J. V. Waszczak, K. M. Young, N. M.
325 Zimmerman, *J. Am. Chem. Soc.*, 1991, **113**, 582–
- 326 19. J. M. Cole, C. M. Aherne, J. A. K. Howard, A. J. Banister, P. G. Waddell, *Acta Crystallogr., Sect. E: Struct. Rep.*
327 *Online*, 2011, **67**, o2514.
- 328 20. J. M. Cole, C. M. Aherne, P. G. Waddell, A. J. Banister, A. S. Batsanov, J. A. K. Howard, *Polyhedron*, 2012,
329 **45**, 61–70.
- 330 21. Y. Beldjoudi, D. A. Haynes, J. J. Hayward, W. J. Manning, D. R. Pratt, J. M. Rawson, *CrystEngComm*, 2013,
331 **15**, 1107–1113.
- 332 22. R. T. Boeré, K. H. Mook, S. Derrick, W. Hoogerdijk, K. Preuss, J. Yip and M. Parvez, *Can. J. Chem.*, 1993, **71**,
333 473–486.
- 334 23. H. F. Lau, P. C. Y. Ang, V. W. L. Ng, S. L. Kuan, L. Y. Goh, A. S. Borisov, P. Hazendonk, T. L. Roemmele, R. T.
335 Boeré and R. D. Webster, *Inorg. Chem.* 2008, **47**, 632–644.
- 336 24. G. M. Sheldrick, *Acta Crystallogr. Sect. A, Found. Adv.*, 2015, **71**, 3–8.
- 337 25. E. A. Adams, J. W. Kolis and W. T. Pennington, *Acta Cryst.* 1990, **C46**, 917–919.
- 338 26. Effendy, W. J. Grigsby, R. D. Hart, C. L. Raston, B. W. Skelton and A. H. White, *Aust. J. Chem.*, 1997, **50**,
339 675–682.
- 340 27. I. Dance and M. Scudder, *Chem. Eur. J.*, 1996, **2**, 481–486.
- 341 28. C. S. Clarke, D. A. Haynes, J. N. B. Smith, A. S. Batsanov, J. A. K. Howard, S. I. Pascu and J. M. Rawson,
342 *CrystEngCom*, 2010, **12**, 172–185.
- 343 29. A. J. Banister, A. S. Batsanov, O. G. Dawe, P. L. Herbertson, J. A. K. Howard, S. Lynn, I. May, J. N. B. Smith, J.
344 M. Rawson, T. E. Rogers, B. K. Tanner, G. Antorrena, F. Palacio, *J. Chem. Soc., Dalton Trans.*, 1997, 2539–
345 2341.

- 346 30. L. Beer, A. W. Cordes, D. J. T. Myles, R. T. Oakley, N. J. Taylor, *CrystEngComm*, 2000, **2**, 109-114.
- 347 31. M. P. Andrews, A. W. Cordes, D. C. Douglass, R. M. Fleming, S. H. Glarum, R. C. Haddon, P. Marsh, R. T.
- 348 Oakley, T. T. M. Palstra, L. F. Schneemeyer, G. W. Trucks, R. Tycko, J. V. Waszczak, K. M. Young, N. M.
- 349 Zimmerman, *J. Am. Chem. Soc.*, 1991, **113**, 3559-3568.
- 350 32. R. A. Beekman, R. T. Boéré, K. H. Moock, M. Parvez, *Can. J. Chem.*, 1998, **76**, 85-93.
- 351 33. A. W. Cordes, R. C. Haddon, R. G. Hicks, R. T. Oakley, T. T. M. Palstra, L. F. Schneemeyer, J. V. Waszczak, J.
- 352 *Am. Chem. Soc.*, 1992, **114**, 5000-5004.
- 353 34. C. P. Constantinides, D. J. Eisler, A. Alberola, E. Carter, D. M. Murphy, J. M. Rawson, *CrystEngComm* (2014),
- 354 16, 7298-.
- 355 35. M. Fedurco, M. M. Olmstead and W. R. Fawcett, *Inorg. Chem.*, 1995, **34**, 390-392.
- 356 36. R. T. Boéré, R. T. Oakley and R. W. Reed, *J. Organomet. Chem.* 1987, **331**, 161-167.
- 357 37. Bruker (2008). *APEX2, SAINT-Plus and SADABS*. Bruker AXS Inc., Madison Wisconsin, USA.
- 358 38. G. M. Sheldrick, *Acta Crystallogr. Sect. A, Found. Crystallog.*, 2008, **64**, 112-122.
- 359 39. G. M. Sheldrick, *Acta Crystallogr. Sect. C, Struct. Chem.*, 2015, **71**, 3-8.
- 360 40. A. Thorn, B. Dittrich and G. M. Sheldrick, *Acta Crystallogr. Sect. A, Found. Crystallog.*, 2012, **68**, 448-451.
- 361 41. D. F. Macrae, P. R. Edgington, P. McCabe, E. Pidcock, G. P. Shields, R. Taylor, M. Towler and J. van de
- 362 Streek, *J. Appl. Cryst.*, 2006, **39**, 453-457.
- 363 42. Gaussian 03, Revision C.02, M. J. Frisch, G. W. Trucks, H. B. Schlegel, G. E. Scuseria, M. A. Robb, J. R.
- 364 Cheeseman, J. A. Montgomery, Jr., T. Vreven, K. N. Kudin, J. C. Burant, J. M. Millam, S. S. Iyengar, J. Tomasi,
- 365 V. Barone, B. Mennucci, M. Cossi, G. Scalmani, N. Rega, G. A. Petersson, H. Nakatsuji, M. Hada, M. Ehara,
- 366 K. Toyota, R. Fukuda, J. Hasegawa, M. Ishida, T. Nakajima, Y. Honda, O. Kitao, H. Nakai, M. Klene, X. Li, J. E.
- 367 Knox, H. P. Hratchian, J. B. Cross, V. Bakken, C. Adamo, J. Jaramillo, R. Gomperts, R. E. Stratmann, O.
- 368 Yazyev, A. J. Austin, R. Cammi, C. Pomelli, J. W. Ochterski, P. Y. Ayala, K. Morokuma, G. A. Voth, P.
- 369 Salvador, J. J. Dannenberg, V. G. Zakrzewski, S. Dapprich, A. D. Daniels, M. C. Strain, O. Farkas, D. K. Malick,
- 370 A. D. Rabuck, K. Raghavachari, J. B. Foresman, J. V. Ortiz, Q. Cui, A. G. Baboul, S. Clifford, J. Cioslowski, B. B.
- 371 Stefanov, G. Liu, A. Liashenko, P. Piskorz, I. Komaromi, R. L. Martin, D. J. Fox, T. Keith, M. A. Al-Laham, C. Y.
- 372 Peng, A. Nanayakkara, M. Challacombe, P. M. W. Gill, B. Johnson, W. Chen, M. W. Wong, C. Gonzalez, and
- 373 J. A. Pople, Gaussian, Inc., Wallingford CT, 2004.
- 374 43. J. C. Collings, K. P. Roscoe, R. L. Thomas, A. S. Batsanov, L. M. Stimson, J. A. K. Howard and T. B. Marder,
- 375 *New J. Chem.*, 2001, **25**, 1410-1417.
- 376 44. S. K. Pal, M. E. Itkis, F. S. Tham, R. W. Reed, R. T. Oakley, B. Donnadiou and R. C. Haddon, *J. Am. Chem. Soc.*,
- 377 2007, **129**, 7163-7174.
- 378 44. Pradip Bag, Mikhail E. Itkis, Dejan Stekovic, Sushanta K. Pal, Fook S. Tham, and Robert C. Haddon, *J. Am.*
- 379 *Chem. Soc.*, 2015, **137**, 10000-10008, and references therein.
- 380
- 381